Journal of Colloid and Interface Science 433 (2014) 149–155

Contents lists available at ScienceDirect

Journal of Colloid and Interface Science

www.elsevier.com/locate/jcis

Catalytic performance of activated carbon supported cobalt catalyst for CO_2 reforming of CH_4

Guojie Zhang *, Aiting Su, Yannian Du, Jiangwen Qu, Ying Xu

Key Laboratory of Coal Science and Technology, Ministry of Education and Shanxi Province, Taiyuan University of Technology, Taiyuan 030024, PR China

ARTICLE INFO

Article history:
Received 22 January 2014
Accepted 15 June 2014
Available online 22 June 2014

Keywords:
Activated carbon
Cobalt
Syngas
CO_2 reforming of CH_4

ABSTRACT

Syngas production by CO_2 reforming of CH_4 in a fixed bed reactor was investigated over a series of activated carbon (AC) supported Co catalysts as a function of Co loading (between 15 and 30 wt.%) and calcination temperature (T_c = 300, 400 or 500 °C). The catalytic performance was assessed through CH_4 and CO_2 conversions and long-term stability. XRD and SEM were used to characterize the catalysts. It was found that the stability of Co/AC catalysts was strongly dependent on the Co loading and calcination temperature. For the loadings (25 wt.% for T_c = 300 °C), stable activities have been achieved. The loading of excess Co (>wt.% 25) causes negative effects not only on the performance of the catalysts but also on the support surface properties. In addition, the experiment showed that ultrasound can enhance and promote dispersion of the active metal on the carrier, thus improving the catalytic performance of the catalyst. The catalyst activity can be long-term stably maintained, and no obvious deactivation has been observed in the first 2700 min. After analyzing the characteristics, a reaction mechanism for CO_2 reforming of CH_4 over Co/AC catalyst was proposed.

1. Introduction

Syngas is a fuel gas mixture consisting primarily of hydrogen, carbon monoxide. Syngas can be used in the Fischer–Tropsch process to produce diesel, or converted into e.g. methane, methanol, and dimethyl ether in catalytic processes [1,2]. Production methods include steam reforming of natural gas or liquid hydrocarbons to produce hydrogen, the gasification of coal, biomass, and some types of waste-to-energy gasification facilities.

Carbon dioxide reforming (also known as dry reforming) is a method of producing syngas (mixtures of hydrogen and carbon monoxide) from the reaction of carbon dioxide with hydrocarbons such as methane. Synthesis gas is conventionally produced via the steam reforming reaction. In the recent years, increased concerns on the contribution of greenhouse gases to global warming have increased interest in the replacement of steam as reactant with carbon dioxide.

The dry reforming reaction may be represented by

$$CO_2 + CH_4 \rightarrow 2H_2 + 2CO$$

Thus, two greenhouse gases are consumed and useful chemical building blocks, hydrogen and carbon monoxide, are produced. Current research focuses on CO_2 reforming of CH_4 as the principal process for the production of synthesis gas from natural gas and coke oven gas. This process reduces greenhouse gas emissions, and its products are the main raw materials in the synthesis of liquid fuels (gas to liquid technology, GTL) [1,2]. However, given that the average bond energy of the C—H bond in methane is 4.1×10^5 J/mol and the dissociation energy of CH_3—H is up to 4.3×10^5 J/Mol, the stability of the methane molecule proves to be very strong. Thus, methane cannot be transformed or decomposed unless under high temperature conditions or under the catalysis of a catalyst.

The major issue with this reaction is inevitable deposition of surface carbon and morphology of this surface carbon is a function of the metal used, duration of reaction, temperature of reaction, and activation rate of CO_2. Depending on the morphology of the carbon, the catalyst may or may not show deactivation effect. This carbon formation can be inhibited by choosing appropriate basic support or promoters. Study on the catalyst development of this reaction has been focused on screening a new catalyst to reach higher activity and better stability. Numerous scientific publications reported that all members of group VIII transition metals with the exception of osmium especially Ni, Ru, Rh, Pd, Ir, and Pt perform an activity to this reaction [1–6]. Among these metals, noble metals have been shown high activity and resistant carbon deposition in CO_2 reforming of CH_4. However, based on economical

* Corresponding author. Fax: +86 351 601 8676.
E-mail addresses: zhgjdoc@126.com, zhangguojie@tyut.edu.cn (G. Zhang).

http://dx.doi.org/10.1016/j.jcis.2014.06.038
0021-9797/

view, upscale toward industrial level of noble metals is not suitable considering their high cost and restricted availability, while Ni- and Co-based catalysts are easily available [7]. The supported nickel is commonly studied because of its low cost and better availability. However, the supported nickel catalyst has a major problem such as carbon deposition and leads to deactivation of the catalyst and/or a plugging of the tubes [8–11]. Because of that reason, it is impossible to avoid carbon formation under low or unity CO_2/CH_4 ratios using nickel catalyst. Recently, although not a focus of attention, it has been revealed that the supported cobalt catalyst shows considerable activity for dry reforming of methane process. Even though the catalytic performance, such as activity is neither superior to nickel nor superior to the noble metal catalyst, study on the supported cobalt catalysts was also reported to find out the better catalytic performance. It is also probable that the mechanism of carbon deposition on cobalt metal is different from that on nickel metal.

Budiman reported the surface features and catalytic performance of supported cobalt catalysts for CO_2 reforming of CH_4 [12]. It was found that 9.0% Co/Al_2O_3 catalyst exhibited optimal catalytic activity, while lots of large Co_3O_4 crystal particles formed which could lead to decay in activity quickly due to carbon deposition. Adding additives can slightly affect catalytic activity. The research has found that the Co/SiO_2 catalyst prepared from cobalt acetate demonstrates the best catalytic activity and stability [13]. This catalyst is significantly different in many ways, such as existence of Co species, metal-support interactions, Co particle size and resistance to sintering and coking. The investigation has found that 9.0 wt.% (or more) Co/Al_2O_3 catalyst calcined at 800–1200 °C not only exhibited high catalytic activity, but also showed optimal resistance to carbon deposition [12,13]. It is Co and $CoAl_2O_4$ that play a very important role in the reaction, and there are many different catalytic features between calcined at high temperature and at low temperature. In summary, Co metal has high catalytic activity, and can form moderately granular crystal after calcination [13–17]. However, the catalyst life is still short. Choosing appropriate catalyst support can lead to synthesis of a catalyst with enhanced resistance to deactivation due to carbon formation by decreasing the formation of carbon. A number of supports for these active metals have also been investigated; Cobalt catalyst deactivated rapidly when the conventional supports, such as Al_2O_3 and SiO_2, were employed.

The author has found that carbon materials (activated carbon) can be used as a carrier. According to previous studies, carbon materials have a certain catalytic ability for CO_2 reforming of CH_4 to syngas [18,19]. Carbon materials have a series of advantages, including low cost, rich pore structure, large specific surface area, and excellent adsorption performance as a carrier [19]. These advantages favor the improvement of catalytic stability. Metal-supported on the carbon carrier is easily recycled by combustion. Moreover, the surface area, pore structure, and surface functional groups of activated carbon play a very important role in the reaction. In this paper, Co/AC catalyst was prepared by impregnation method from $Co(NO_3)_2$ as active precursor, AC as a carrier. The effects of cobalt salt on catalyst structure and performance on CO_2 reforming of CH_4 are investigated using activity evaluation as well as XRD, SEM and BET techniques. In addition, the reaction mechanism is also important to be explained.

2. Experimental

2.1. Catalyst preparation

A heterogeneous cobalt catalyst was prepared by wetness impregnation of cobalt ion on an activated carbon (AC). The activated carbon carrier (15–35 mesh) was impregnated with a solution containing the required amount of $Co(NO_3)_2{\cdot}6H_2O$ for 12 h. The obtained solid was dried at 110 °C for 4 h, and then calcined at 400 °C for 4 h. Finally, the catalyst was reduced in a tube furnace at 400 °C with H_2 (100 ml/min) for 4 h. Ultrasonic impregnation was carried out by placing the mixture of active carbon carrier and a solution containing the required amount of $Co(NO_3)_2{\cdot}6H_2O$ in an ultrasonic cleaning machine at a frequency of 40 kHz for 10 min. After the mixture was allowed to stand for 12 h, the obtained solid was dried, calcined and reduced. Table 1 shows the proximate and ultimate analyses of active carbon.

2.2. Catalytic activity measurements

Catalytic activity measurements were taken at an atmospheric pressure in a 20 mm diameter continuous flow quartz reactor using 100 mg of catalyst material. After heating for a given set-point, CH_4/CO_2 mixture ($CH_4/CO_2 = 1$) was introduced into the reactor. The gas hourly space velocity (GHSV) was 720 h^{-1}. After reaching steady-state conditions, the mixture of reactant gases and products was periodically analyzed by a gas chromatography. The C, H, and O balance across the reactor was more than 97%. All experiments with larger errors in the material balances were rejected. Prior to analysis, the effluent was passed through a water-trap at 0 °C in order to remove reaction water. The calculation equation of CH_4 and CO_2 conversion was followed:

$$X_{CH_4} = \frac{F_{CH_4\ in} \times Y_{CH_4\ in} - F_{CH_4 out} \times Y_{CH_4 out}}{F_{CH_4 in} \times Y_{CH_4\ in}} \times 100\%$$

$$X_{CO_2} = \frac{F_{CO_2 in} \times Y_{CO_2 in} - F_{CO_2 out} \times Y_{CO_2 out}}{F_{CO_2 in} \times Y_{CO_2 in}} \times 100\%$$

where X is the conversion of the CH_4 or CO_2, V/V; F is the gas flow rate of in and out, ml min^{-1}; Y is different fraction volume percentages; superscript in is the inlet; superscript out is the outlet.

2.3. Characterization of catalyst

The crystalline structures of the catalysts were determined by X-ray powder diffraction (XRD) with a computer-controlled Dandong DX-2700 apparatus equipped with a monochromator for the Cu Ka radiation (Cu Kα, $\lambda = 0.154$ nm), operating at 40 kV and 30 MA. Spectra were scanned in the range from 10° to 80°. Scanning speed was 8°/min under atmospheric pressure. Morphology of the catalyst sample was observed by JSM-6700F type scanning electron microscope (FESEM, the acceleration voltage of 0.5–30 kV, resolution was 1.0 nm (15 kV)/2.2 nm (1 kV)). The catalyst samples were deposited on thin amorphous carbon films supported by copper grids. The BET specific surface area of the catalysts was analyzed with a Sorptmantic 1990 instrument using nitrogen as adsorbed at 77 K.

3. Results and discussion

3.1. Effects of impregnation amount

A series of Co/AC catalysts were prepared by wetness impregnation from different content cobalt salt (15 wt.%, 20 wt.%, 25 wt.% and 30 wt.%) precursors for CO_2 reforming of CH_4. Effects of the impregnation amount on the catalyst activity are shown in Figs. 1 and 2. It was found that the order of catalytic activity of the different loading amounts of Co/AC catalyst is 25% > 30% > 20% > 15%. There is a decrease in surface area of Co impregnated activated carbon versus neat activated carbon (Table 2). The decrease in the surface area could indicate that there was some amount of Co blocking

Table 1
Proximate analysis and ultimate analysis of AC.

Sample	Proximate analysis, wt.%, ad			Ultimate analysis, wt.%, daf				
	Moisture	Ash	Volatile matter	C	H	N	S	O (diff)
Activated carbon	1.30	7.67	1.72	80.59	0.91	0.35	0.50	0.35

ad: Air dried; daf: dry ash free; diff: difference.

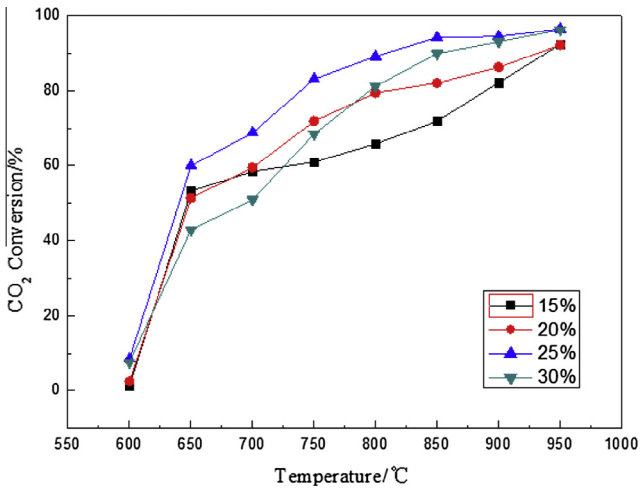

Fig. 1. Effects of impregnation amount on CO_2 conversion (reaction conditions: gas flow rate: 120 ml min^{-1}, pressure: 0.1 MPa, CH_4/CO_2 = 1:1).

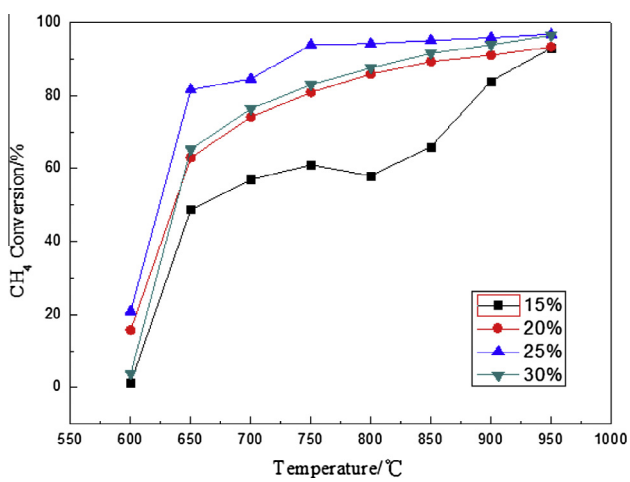

Fig. 2. Effects of impregnation amount on CH_4 conversion (reaction conditions: gas flow rate: 120 ml min^{-1}, pressure: 0.1 MPa, CH_4/CO_2 = 1:1).

Table 2
Pore structure characteristics of AC and Co/AC.

Sample	A_{BET} (m^2/g)	V_P (cm^3/g)	d_P (nm)
AC sample	951.38	0.64	2.79
15% Co/AC	802.46	0.52	2.78
20% Co/AC	726.52	0.48	2.76
25% Co/AC	648.97	0.46	2.75
30% Co/AC	646.35	0.43	2.65
25% Co/AC (after reaction)	645.70	0.43	2.71

the micro-pore which resulted in a decrease in pore volume. The result supported the SEM morphology that there was hardly change in the surface morphology (Fig. 3). However, from the result it can be assumed that 25 wt.% Co did not entirely load into the pore site of the activated carbon because there was only a slight decrease in the pore volume. As Co loading increases, the catalytic activity of the catalyst increases until the saturation point reached. The micro-porous structure of the carbon surface is blocked when Co loading exceeds the saturation point [12–17]. It is not conducive to gas molecule adsorption and activation. In addition, the number of reactive sites on the carrier surface decreases with Co loading up to the saturation point. Both reasons result in reduced catalytic activity of the catalyst.

SEM images of different Co/AC catalysts are given in Fig. 3. It was found that there is not Co cluster formation at low cobalt loadings. However, at cobalt loading up to 25 wt.%, it was found that the excess Co started agglomerates. At higher Co loading, excessive Co forms clusters on the catalyst surface and blocks the pores (as shown in Fig. 3(B) and Table 2), the surface area and the micro-pore amount of catalyst decreases. The preferred impregnation is 25 wt.%.

3.2. Effects of calcination temperature

Calcination is an important factor for catalyst preparation. It is a thermal treatment process in the presence of air or oxygen applied to ores and other solid materials to bring about a thermal decomposition, phase transition, or the removal of a volatile fraction. Reactions of calcination processes include the following: decomposition of carbonate minerals; decomposition of hydrated minerals, to remove crystalline water as water vapor; decomposition of volatile matter contained in raw petroleum coke; and heat treatment to effect phase transformations. Samples from the same raw material (precursor) are converted into different products by variation in the batch size during calcination. The effect of calcination temperature (300 °C, 400 °C and 500 °C) on the catalytic activity for CO_2 reforming of CH_4 to syngas was investigated for Co/AC catalysts, as shown in Figs. 4 and 5. The results show that the catalysts exhibit the same catalytic trend under the three calcination temperature. As the reaction temperature increases, the conversion of methane and carbon dioxide gradually increases. At 950 °C reaction temperature, the conversions of methane were 98.4 v/v% (300 °C calcination) and 93.3 v/v% (500 °C calcination); whereas the conversions of carbon dioxide were 97.1 v/v% (300 °C calcination)and 92.7 v/v% (500 °C calcination). It was found that with increasing calcination temperatures, catalyst activity decreases. Catalyst activity has a sharp decrease at 500 °C. The optimal calcination temperature for the Co/AC was 300 °C. This may be caused by the direct effect of calcination temperature on the crystal structure of active components. According to calcination mechanism, sintering is generated immediately upon the collision and concentration of crystals, which is controlled by the diffusion and migration of active components. Component calcination under 300 °C may be easier to be restored. Under high calcination temperature, sintering of the catalyst become more serious as time goes on. Smaller particles aggregate to form larger particles; surface area can decrease drastically [20].

XRD was carried out on all samples to identify the species formed in the samples. Fig. 6 presents the XRD patterns of catalysts with different calcination temperatures. According to the standard

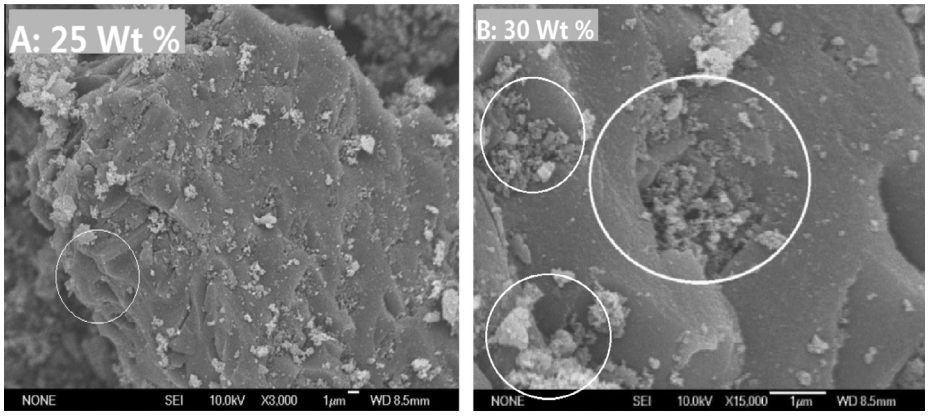

Fig. 3. SEM image of the catalyst.

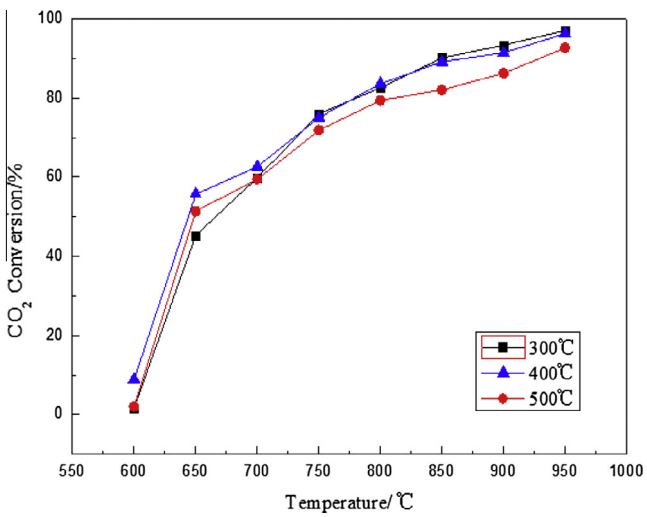

Fig. 4. Effects of calcination temperature on CO_2 conversion.

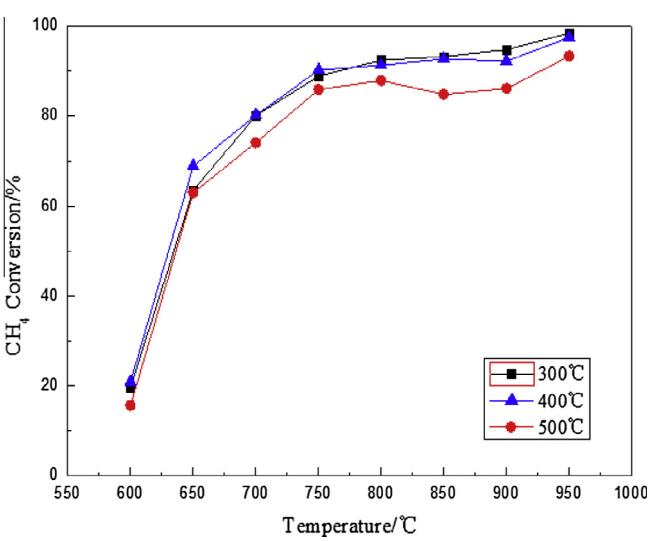

Fig. 5. Effect of calcination temperature on CH_4 conversion (impregnation amount: 25 wt.%).

map [21,22], the diffraction peak at 26.6° is contributed by graphite; the diffraction peak at 43.4° is contributed by Co. The intensity of the diffraction peaks is different between the catalysts prepared

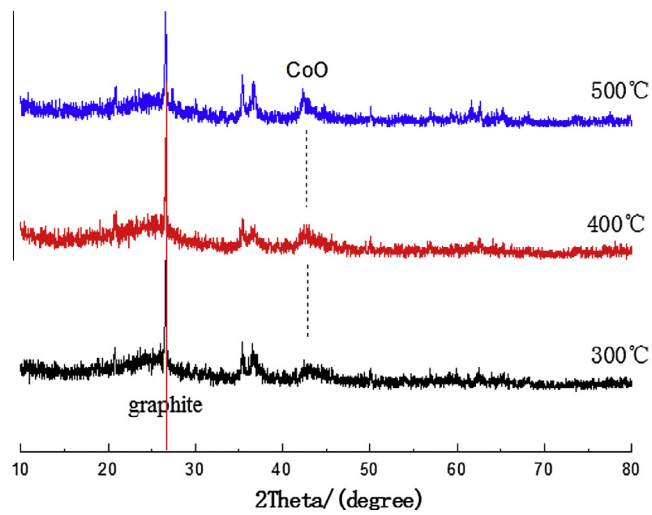

Fig. 6. XRD patterns of catalyst under different calcination temperature.

from different calcination temperatures. The intensity of the cobalt oxide diffraction peak of the 500 °C calcination catalyst is higher than that of the catalyst prepared at 300 °C calcination. This result suggests that the different calcination temperatures affect the growth of cobalt metal oxide crystals. Too high calcination temperature will promote the growth of the cobalt oxide crystals, and sintering is also generally accelerated. Hence, a higher degree of cobalt oxide crystallinity is formed. It is not conducive to the reduction to cobalt metal. As a result, the active substance content of the catalyst reduces; catalytic activity of catalyst decreases. The diffraction peak intensity of cobalt oxide (XRD pattern) in the catalyst calcined at 300 °C is weak. It indicates that the cobalt oxide is highly dispersed on the active carbon surface, and the crystallinity is a moderate.

3.3. Effect of the ultrasonic wave

Ultrasonic cavitation is a series of dynamic processes that generate tensile stress when the ultrasonic wave spreads in the liquid. At the same time, it forms a negative pressure in the partial liquid. Thus, the original micro-bubble expands until it bursts, and then the surrounding liquid breaks into the bubble with high temperature, high pressure, shock, and strong noise. This study selected 40 kHz of ultrasonic treatment for 10 min to investigate the effect of ultrasonic impregnation on catalyst performance.

The activity of the catalyst prepared by ultrasonic impregnation is significantly higher than that of the catalyst prepared by conventional impregnation, as shown in Figs. 7 and 8. CO_2 and CH_4 conversions are 98 v/v% and 97 v/v% over the catalyst prepared by ultrasonic impregnation treatment; whereas CO_2 and CH_4 conversions are 95 v/v% and 94 v/v% over the catalyst prepared by conventional impregnation, respectively. It is mainly due to the fact that distribution of the active substance on the carrier surface is more uniformly after ultrasonic treatment. The distribution differences in the active substance on the carrier surface are shown in Fig. 9. The distribution of active substance on the ultrasonically impregnated catalyst surface is more uniform than that on the ordinarily impregnated catalyst surface. These differences are mainly caused by three reasons. First, in the static impregnation process, the driving force for mass transfer is mainly the active substance concentration gradient between the vicinity of the carrier surface solution and the active substance of the solution. In the ultrasonic impregnation process, the particle obtains great acceleration and kinetic energy by the ultrasonic vibration, which can accelerate the active substance diffusion motion and increase the active ingredient the mass transfer driving force. Eventually, it improves the mass transfer rate. Second, the high-pressure shock wave generated by ultrasonic cavitation affects the pore structure of the carrier. This shock wave may cause the collapse of the macro-porous and generate more micro-pores, thereby increasing surface area of catalyst. It can adsorb more amounts of active substance and gas molecules, and improve the chance of the activation of methane and carbon dioxide. Third, ultrasonic cavitation suppresses the formation of active substance soft agglomerates. Addition of ultrasonic wave can disperse active component of catalyst, then enhance the dispersion of the active component, therefore decrease the active group forming carbon-deposition, and as a result, improve the resistance to carbon deposition. At the same time, enhancement of dispersion is beneficial to the improvement of catalytic activity. On the other hand, eliminating carbon-deposition in time promotes the turnover frequency of the active site, thereby speeding up conversion of CH_4 and CO_2. Report obtained the same conclusion on this topic [23].

3.4. Life cycle assessment

Fig. 10 shows the effect of time-on-stream on the CO_2 reforming of CH_4 at 950 °C over Co (25 wt.%)/AC and Ni/Al_2O_3 catalysts. The Co/AC catalyst maintained high catalytic activity for 2700 min.

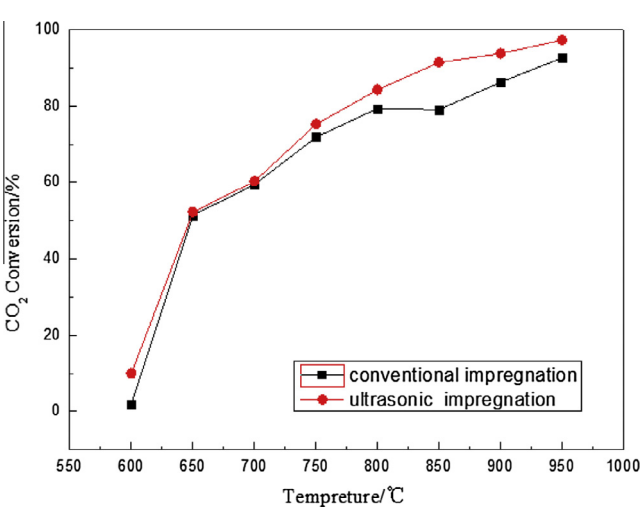

Fig. 7. Effect of ultrasonic treatment on CO_2 conversion (impregnation amount: 25 wt.%, calcination temperature: 300 °C).

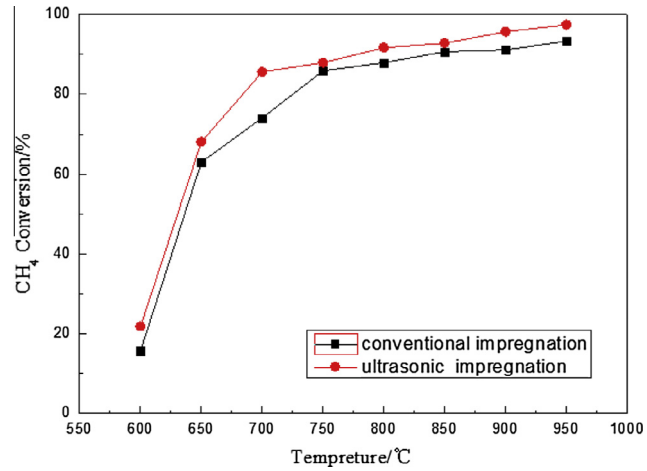

Fig. 8. Effect of ultrasonic on CH_4 conversion (impregnation amount: 25 wt.%, calcination temperature: 300 °C).

After reforming, no carbon deposition was observed on the Co/AC catalyst. On the other hand, the Ni/Al_2O_3 catalyst showed gradual deactivation over a period of 2700 min. The primary technical problem of metal-loaded catalysts is the formation of carbon deposition on the catalysts, which may plug the reformer tubes. Different supports affect the resistance to carbon-deposition of catalysts differently. This phenomenon may be attributed to two reasons. First, the activated carbon carrier has a large surface area, on which the cobalt oxide is uniformly dispersed. Second, the activated carbon carrier has many C=O, —CO—, and oxygen-containing functional groups [19,24,25]. In the Co/AC catalyst, an oxygen species with higher reactivity existed near active species, which seemed to promote oxidation of the catalyst surface [19]. The oxygen in the carbonaceous material includes the polar state and non-polar state, such as OH group, carboxyl group and phenolic hydroxyl group whose polarity is strong. Zhang et al. [26] reported that the different oxygen species makes the nature of electrical energy on the surface different; the catalytic activity depends on the polarity of oxygen from different species. The oxygen in the anhydride and lactone structures on the surface of carbonaceous materials is active oxygen, which is the main active component and associate with H in methane molecules as the dipole force, and it can reduce the activation energy of methane dehydrogenation. In addition, they can change the shape and concentration of the electron cloud in C—H bond under the action of oxygen atom charge, and promote the fracture of C—H bond to generate highly active CH_3^* ions. These ions ultimately form CO and H_2. It may be an important factor in increasing catalytic stability.

3.5. Proposed mechanism of drying reforming over Co/AC catalyst

The catalytic activity of carbon catalysts for CO_2 reforming of CH_4 is also previewed at home and abroad. In general, the dry reforming reaction can be considered as a combination of CH_4 decomposition and gasification of the carbon deposits by CO_2. In addition, it was also demonstrated that the surface oxygen functional groups participated in the reforming reaction [21,23,26]. CO_2 reforming of CH_4 over Co/AC catalyst was studied and the proposed mechanism is as follows.

Firstly, CH_4 could undergo a dissociative adsorption on the catalyst surface. Then the reactive carbonaceous deposits from CH_4 decomposition are gasified by CO_2. The active metal M on the catalyst reduces the dissociation energy barrier of methane, thus triggering a chain effect. The cobalt grains and methane molecules adsorbed form cobalt–carbon compound intermediates, which

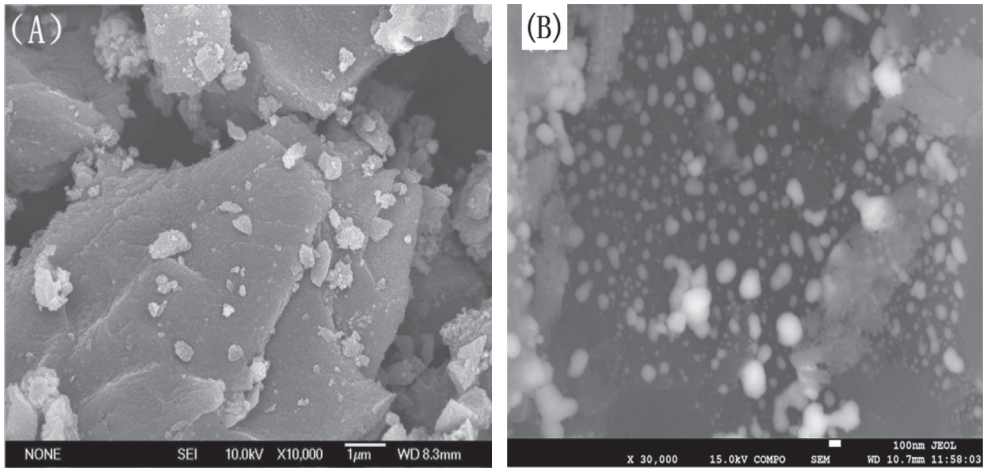

Fig. 9. SEM images ((A) conventional impregnation; (B) ultrasonic impregnation).

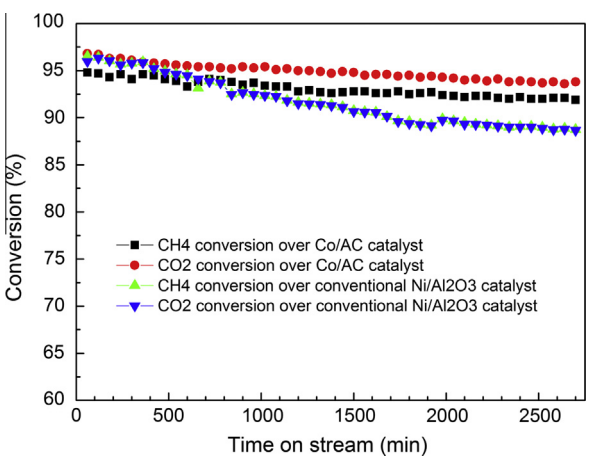

Fig. 10. Life of catalyst (reaction temperature: 950 °C).

are combined through a certain bonding action. Then, the intermediate dissociates to form H^*; carbon dioxide is rapidly activated by H^* to generate OH^*. OH^* reacts with CHx–M. The detailed reaction course is as follows.

$$CH_4 + M \rightarrow CH_x - M + (4 - X)H^* \quad (1)$$
$$CO_2 + H^* \rightarrow CO + OH^* \quad (2)$$
$$CH_X - M + OH^* \rightarrow CH_XO^* + H - M \quad (3)$$
$$CH_XO^* \rightarrow CO + XH^* \quad (4)$$
$$CH_x - M \rightarrow C + M - H_X \quad (5)$$
$$CO_2 + C \rightarrow 2CO \quad (6)$$
$$M - H_X \rightarrow M + XH^* \quad (7)$$
$$H - M \rightarrow M + H^* \quad (8)$$
$$XH^* \rightarrow X/2H_2 \quad (9)$$

The hydrogen atoms form hydrogen, and the active material M is recycled for reuse. Two reactions of methane pyrolysis and carbon dioxide activation can be speculated to be mutually reinforcing each other. These reactions belong to the same reaction rate controlling step.

Secondly, the surface of the activated carbon contains abundant surface functional groups, such as hydroxyl, carboxyl, anhydride, ether and quinone radicals, which has an effect on the catalyst activity. These Oxygen-containing functional groups can make the electron cloud shape and concentration distribution of the C—H bond in CH_4 be changed. CH_4 adsorption and dissociative over oxygen functional groups are the rate-determining step. CH_4 dehydrogenates to form CH_X^* and H^*. Subsequently, the obtained H^* is converted into OH^*, O^* and H_2. CO_2 and H^* are converted into CO and OH^*. The processes of methane modular activation by oxygen functional groups are as follows:

$$R{-}C{=}O + CH_4 \rightarrow R{-}C{=}O \ldots H{-}CH3 \rightarrow R{-}C{=}O + H^* + CH_3^* \quad (10)$$
$$CO_2 + H^* \rightarrow CO + OH^* \quad (11)$$
$$2OH^* \rightarrow H_2O + O^* \quad (12)$$
$$CH_4 + O^* \rightarrow CH_3^* + OH^* \quad (13)$$
$$CH_3^* + (3 - X)^* \rightarrow CHx^* + (3 - X)H^* \quad (14)$$
$$CHx^* + O^* \rightarrow CO + XH^* \quad (15)$$
$$CHx^* + CO_2 \rightarrow 2CO + XH^* \quad (16)$$
$$XH^* \rightarrow X/2H_2 \quad (17)$$

4. Conclusions

The results show that 25 wt.% Co/AC catalyst displayed the highest activity and stability for CO_2 reforming of CH_4. The loading of excess Co (>wt.% 25) causes negative effects not only on the performance of the catalysts but also on the support surface properties. It was not favorable for the adsorption of the gas. The optimal calcination temperature for the Co/AC catalyst was 300 °C. The result shows that the catalyst presented a good degree of crystallinity and had better anti-sintering ability and coking resistance ability after calcination at 300 °C. Additional ultrasonic wave can enhance and promote dispersion of the active metal on the carrier, thus improving the catalytic performance of the catalyst. By optimizing the metal loading (25 wt.% for T_c = 300 °C), highly effective and stable Co/AC catalysts can be obtained. The catalyst activity can be long-term stably maintained, no obvious deactivation has been observed in 2700 min. These results suggest that cobalt catalyst is a potential alternative among non-noble metal catalysts. A simple reaction mechanism for CO_2 reforming CH_4 over a Co/AC catalyst is proposed after analyzing the characteristics of the catalyst.

Acknowledgments

This work was supported by the National Science & Technology Pillar Program (Grant No. 2012BAA04B03), Natural Science

Foundation of China (Grant Nos. 21006066 and 51274147), STIP, OIT and Shanxi Provincial Natural Science Foundation (Grant No. 2011021009-2).

References

[1] S. Gaur, D. Pakhare, H. Wu, Energy Fuels 26 (2012) 1989–1998.
[2] H. Li, Q. Xu, D. Zhang, Adv. Mater. Res. 356–360 (2011) 1070–1074.
[3] S. Tada, R. Kikuchia, K. Urasakib, Appl. Catal. A: Gen. 404 (2011) 149–154.
[4] M. Ocsachoque, J. Bengoa, D. Gazzoli, Catal. Lett. 141 (2011) 1643–1650.
[5] P. Djinovic, I.G.O. Crnivec, J. Batista, J. Levec, A. Pintar, Chem. Eng. Process: Process Intens. 50 (2011) 1054–1062.
[6] I. Sarusi, K. Fodor, K. Baan, Catal. Today 171 (2011) 132–139.
[7] G. Zhang, Y. Du, Y. Xu, Y. Zhang, J. Ind. Eng. Chem. 20 (2014) 1677–1683.
[8] M.A. Naeem, A.S. Al-Fatesh, W.U. Khan, A.E. Abasaeed, A.H. Fakeeha, Int. J. Chem. Eng. Appl. 4 (2013) 315–320.
[9] M.H. Amin, K. Mantri, J. Newnham, J. Tardio, S.K. Bhargava, Appl. Catal. B: Environ. 119–120 (2012) 217–226.
[10] D. Cheng, X. Zhu, Y. Ben, Catal. Today 115 (2006) 205–210.
[11] Z. Hao, Q. Zhu, Z. Lei, Powder Technol. 179 (2007) 157–162.
[12] A.W. Budiman, S.H. Song, T.S. Chang, C.H. Shin, M.J. Choi, Catal. Surv. Asia 16 (2012) 183–197.
[13] D. Pakhare, J. Spivey, Soc. Rev. (2014), http://dx.doi.org/10.1039/C3CS60395D.
[14] K. Nakagawa, M. Kikuchi, M. Nishitani-Gamo, H. Oda, H. Gamo, K.I. Ogawa, T. Ando, Energy Fuels 22 (2008) 3566–3570.
[15] S. Zeng, L. Zhang, X. Zhang, Y. Wang, H. Pan, H. Su, Int. J. Hydrogen Energy 37 (2012) 9994–10001.
[16] K. Takanabe, K. Nagaoka, K. Nariai, K. Aika, J. Catal. 230 (2005) 75–85.
[17] V.Y. Bychkov, Y.P. Tyulenin, O.V. Krylov, V.N. Korchak, Kinet. Catal. 43 (2002) 724–730.
[18] G. Zhang, Y. Dong, M. Feng, Y. Zhang, W. Zhao, H. Cao, Chem. Eng. J. 56 (2010) 519–523.
[19] G. Zhang, J. Qu, Y. Du, F. Guo, H. Zhao, Y. Zhang, Y. Xu, J. Ind. Eng. Chem. 20 (2014) 2948–2957.
[20] Y. Xu, Z. Liu, H. Xia, Catalyst Design and Preparation Process, Chemical Industry Press, Beijing, 2003.
[21] K. Takanabe, K. Nagaoka, K. Nariai, K. Aika, J. Catal. 230 (2005) 75–85.
[22] Z. Wang, H. Wang, Y. Liu, RSC Adv. 3 (2013) 10027–10036.
[23] X. Liang, L. Zhang, H. Ding, Y. Qin, Acta Phys. – Chim. Sin. 19 (2003) 666–669.
[24] F. Guo, Y. Zhang, G. Zhang, H. Zhao, J. Power Sources 231 (2013) 82–90.
[25] W. Zhang, Y. Zhang, Front Chem. Eng. 4 (2010) 147–152.
[26] G. Zhang, J. Qu, A. Su, Y. Zhang, Y. Xu, Towards understanding the carbon catalyzed CO_2 reforming of methane to syngas, J. Ind. Eng. Chem. <http://dx.doi.org/10.1016/j.jiec.2014.02.038>.